

Solubility of Lysozyme in the Presence of Aqueous Chloride Salts: Common-Ion Effect and Its Role on Solubility and Crystal Thermodynamics

Onofrio Annunziata,* Andrew Payne,[†] and Ying Wang

Department of Chemistry, Texas Christian University, Fort Worth, Texas 76129

Received June 6, 2008

Abstract: Understanding protein solubility is important for a rational design of the conditions of protein crystallization. We report measurements of lysozyme solubility in aqueous solutions as a function of NaCl, KCl, and NH₄Cl concentrations at 25 °C and pH 4.5. Our solubility results are directly compared to preferential-interaction coefficients of these ternary solutions determined in the same experimental conditions by ternary diffusion. This comparison has provided new important insight on the dependence of protein solubility on salt concentration. We remark that the dependence of the preferential-interaction coefficient as a function of salt concentration is substantially shaped by the common-ion effect. This effect plays a crucial role also on the observed behavior of lysozyme solubility. We find that the dependence of solubility on salt type and concentration strongly correlates with the corresponding dependence of the preferential-interaction coefficient. Examination of both preferential-interaction coefficients and second virial coefficients has allowed us to demonstrate that the solubility dependence on salt concentration is substantially affected by the corresponding change of protein chemical potential in the crystalline phase. We propose a simple model for the crystalline phase based on salt partitioning between solution and the hydrated protein crystal. A novel solubility equation is reported that quantitatively explains the observed experimental dependence of protein solubility on salt concentration.

Introduction

Protein crystallization is of great importance in several applications such as the determination of protein 3D structure,^{1–8} protein purification,⁹ and the preparation of cross-linked enzyme crystals relevant to the catalysis of petroleum derivatives in nonaqueous media.^{10–12} However, protein crystallization is not well understood and crystals are typically obtained using trial-and-error strategies. One central aspect of this phase transition

is protein solubility in aqueous solution and its dependence on physicochemical parameters such as solution pH, temperature, type, and concentration of precipitants.¹³ Understanding the behavior of protein solubility is not only important for defining the phase-diagram domain in which crystallization may occur but it is also a crucial parameter for the characterization of supersaturation conditions. This is essential for controlling the quality and size of protein crystals, and the competition between protein crystallization and amorphous aggregation.^{1,15,16}

Among all precipitants, salts have been extensively employed to effectively reduce protein solubility and induce crystallization.^{1,13,18,19} Clearly, understanding the dependence of protein solubility on salt concentration is crucial for predicting and designing crystallization conditions. The decrease of protein solubility as salt concentration increases is related to the corresponding increase of protein chemical potential in solution. Hence, thermodynamic investigations on protein solutions play a crucial role in understanding solubility behavior.¹³

Several thermodynamic studies on protein–salt aqueous solutions have been reported. Most of them have focused on

[†] Current address: Department of Pharmacology and Neuroscience, University of North Texas Health Science Center, 3500 Camp Bowie Blvd., Fort Worth, TX 76107.

- (1) McPherson, A. *Crystallization of Biological Macromolecules*; Cold Spring Harbor: New York, 1998.
- (2) Lin, S.-X.; McPherson, A.; Giegé, R. *Cryst. Growth Des.* **2007**, *7*, 2124–2125.
- (3) Anderson, V. J.; Lekkerkerker, H. N. W. *Nature* **2002**, *416*, 811–815.
- (4) Gliko, O.; Neumaier, N.; Pan, W.; Haase, I.; Fischer, M.; Bacher, A.; Weinkauff, S.; Vekilov, P. G. *J. Am. Chem. Soc.* **2005**, *127*, 3433–3438.
- (5) Yau, S.-T.; Vekilov, P. G. *Nature* **2000**, *406*, 494–497.
- (6) Shim, J.-U.; Cristobal, G.; Link, D. R.; Thorsen, T.; Jia, Y.; Piattelli, K.; Fraden, S. *J. Am. Chem. Soc.* **2007**, *129*, 8825–8835.
- (7) Doerr, A. *Nat. Methods* **2006**, *3*, 244.
- (8) Wang, L.; Lee, M. H.; Barton, J.; Hughes, L.; Odom, T. W. *J. Am. Chem. Soc.* **2008**, *130*, 2142–2143.
- (9) Roe, S. *Protein Purification Techniques*; Oxford: Oxford, U.K., 2001.
- (10) Ayala, M.; Vasquez-Duhalt, R. *Enzymatic Catalysis on Petroleum Products*. In *Studies in Surface Science and Catalysis*; Vasquez-Duhalt, R., Quintero-Ramirez, R. Eds.; Elsevier: Amsterdam, 2004; *151*, pp 67–111.
- (11) Margolin, A. L.; Navia, M. A. *Angew. Chem., Int. Ed.* **2001**, *40*, 2204–2222.
- (12) Roy, J. J.; Abraham, T. E. *Chem. Rev.* **2004**, *104*, 3705–3721.

- (13) Arakawa, T.; Timasheff, S. N. *Methods Enzymol.* **1985**, *114*, 49–77.
- (14) Anderson, M. J.; Hansen, C. L.; Quake, S. R. *Proc. Natl. Acad. Sci. USA* **2006**, *103*, 16746–16751.
- (15) Lomakin, A.; Asherie, N.; Benedek, G. B. *Proc. Natl. Acad. Sci. USA* **2003**, *100*, 10254–10257.
- (16) Ducruix, A.; Giegé, R. *Crystallization of Nucleic Acids and Proteins. A Practical Approach*; Oxford University Press: New York, 1992.
- (17) Asthagiri, D.; Paliwal, A.; Abras, A.; Lenhoff, A. M.; Paulaitis, M. E. *Biophys. J.* **2005**, *88*, 3300–3309.
- (18) Zhang, Y.; Cremer, P. S. *Curr. Opin. Chem. Biol.* **2006**, *10*, 658–663.

lysozyme as a model protein. The second virial coefficient, B_2 , determined by light scattering,¹⁷ X-ray scattering,²⁰ and chromatography,²¹ has been the primary parameter for investigating the salt effect on protein–protein interactions. Microscopic models based on the potential of mean force have been used to describe salt-mediated protein–protein interactions.²² Because this approach does not yield direct information on protein–salt interactions, B_2 alone provides only a limited understanding of the thermodynamic behavior of protein–salt solutions. Indeed, although the decrease of B_2 as salt concentration increases correlates with a corresponding decrease of solubility,^{23,24} a quantitative prediction of the dependence of solubility on salt concentration requires the knowledge of protein–salt interactions.^{13,25}

Equilibrium dialysis²⁶ and vapor pressure osmosis²⁷ have been used to characterize protein–salt thermodynamic interactions through the determination of the preferential-interaction coefficient, Γ_{23} . The obtained experimental results have allowed Arakawa and Timasheff to (1) theoretically examine the relation of Γ_{23} to protein solubility,¹³ and (2) show the importance of ion binding and crystal thermodynamics on the behavior protein solubility.²⁸ However, the behavior of Γ_{23} as a function of salt concentration using these experimental techniques has not been assessed in the case of lysozyme. As we shall see in this article, this aspect is critical for understanding the dependence of solubility on salt concentration in the case of charged proteins. Here, it is generally not understood to which extent the behavior of protein solubility is related to preferential hydration compared to common-ion effects and how their relative roles change as a function of salt concentration and type.^{13,29–32}

Recently, a method³³ based on ternary diffusion measurements³⁴ has been introduced for the determination of Γ_{23} . This method has been applied to lysozyme in the presence of chloride salts at 25 °C and pH 4.5.^{34–36} The precision of the obtained thermodynamic data (the determined Γ_{23} values display a typical error of ± 0.2) was found to be crucial for (1) reproducing chloride salt ranking of precipitant effectiveness, (2) quantifying the relative contribution of the common-ion effects and protein

preferential hydration by examining the dependence of Γ_{23} on salt concentration, and (3) for making some important observations regarding the relation between solution thermodynamics and protein solubility.³⁵ These results represent a starting point for a quantitative understanding of the effect of salt concentration on lysozyme solubility.

In this article, we report solubility measurements for lysozyme crystallized in the tetragonal form as a function of salt concentration for three cases: NaCl, KCl, and NH₄Cl at 25 °C and pH 4.5. We quantitatively compare our results with the corresponding Γ_{23} values. Although several solubility studies^{30,37–41} have been reported on lysozyme in aqueous salts, systematic studies on lysozyme solubility at pH 4.5 and 25 °C for all three cases are missing. This is required for performing our proposed quantitative comparison because the Γ_{23} values were obtained in these experimental conditions. Furthermore, we note that the strong dependence of protein–salt interactions on salt concentration plays a crucial role in this comparison. This aspect represents a new and essential addition to previous interpretations of lysozyme solubility. By examining both Γ_{23} and B_2 , we experimentally demonstrate that salt partitioning between solution and protein crystal plays a substantial role on the dependence of solubility on salt concentration. We propose a model that quantitatively describes the observed solubility behavior.

Theory. In this section, we review fundamental thermodynamic relationships between chemical potentials, preferential-interaction coefficients, second virial coefficients, and solubility in isothermal and isobaric conditions. We will consider the case of a positively charged protein with charge Z in the presence of 1:1 electrolytes. The expressions for the chemical potentials, μ_2 (protein, 2) and μ_3 (salt, 3), in solution are^{42–44}

$$\hat{\mu}_2 \equiv (\mu_2 - \mu_2^0)/RT = \ln m_2 + Z \ln(Zm_2 + m_3) + \beta_2 \quad (1a)$$

$$\hat{\mu}_3 \equiv (\mu_3 - \mu_3^0)/RT = \ln m_3 + \ln(Zm_2 + m_3) + \beta_3 \quad (1b)$$

where $\hat{\mu}_i$'s (with $i = 2, 3$) are dimensionless reduced chemical potentials, m_i 's are the solute molalities, β_i 's reduced chemical-potential excesses, μ_i^0 's the standard chemical potentials, R the gas constant, and T the absolute temperature. The first derivatives of the chemical potentials, $\hat{\mu}_{ij} \equiv (\partial \hat{\mu}_i / \partial m_j)_{m_k, k \neq j}$, are directly related to the effect of salt on protein–protein interactions and protein–salt interactions:

$$\hat{\mu}_{22} = \frac{1}{m_2} \left(1 + \frac{Z^2 m_2}{Zm_2 + m_3} + \beta_{22} m_2 \right) \quad (2a)$$

$$\hat{\mu}_{23} = \frac{Z}{Zm_2 + m_3} + \beta_{23} \quad (2b)$$

$$\hat{\mu}_{33} = \frac{1}{m_3} \left(1 + \frac{m_3}{Zm_2 + m_3} + \beta_{33} m_3 \right) \quad (2c)$$

- (19) Vekilov, P. G. *Cryst. Growth Des.* **2007**, *7*, 2239–2246.
 (20) Tardieu, A.; Bonneté, F.; Finet, S.; Vivares, D. *Acta Crystallogr.* **2002**, *D58*, 1549–1553.
 (21) Tessier, P. M.; Lenhoff, A. M. *Curr. Opin. Biotechnol.* **2003**, *14*, 512–516.
 (22) Boström, M.; Tavares, F. W.; Ninham, B. W.; Prausnitz, J. M. *J. Phys. Chem. B* **2006**, *110*, 24757–24760.
 (23) George, A.; Wilson, W. W. *Acta Crystallogr.* **1994**, *D50*, 361–365.
 (24) Guo, B.; Kao, S.; McDonald, H.; Asanov, A.; Combs, L. L.; Wilson, W. W. *J. Cryst. Growth* **1999**, *196*, 424–433.
 (25) Shulgin, I. L.; Ruckenstein, E. *Biophys. Chem.* **2005**, *118*, 128–134.
 (26) Arakawa, T.; Timasheff, S. N. *Biochemistry* **1982**, *21*, 6545–6552.
 (27) Courtenay, E. S.; Capp, M. W.; Anderson, C. F.; Record, M. T., Jr. *Biochemistry* **2000**, *39*, 4455–4471.
 (28) Arakawa, T.; Bath, R.; Timasheff, S. N. *Biochemistry* **1990**, *29*, 1914–1923.
 (29) Benas, P.; Legrand, L.; Ries-Kautt, M. *Acta Crystallogr.* **2002**, *D58*, 1582–1587.
 (30) Retailleau, P.; Ries-Kautt, M.; Ducruix, A. *Biophys. J.* **1997**, *73*, 2156–2163.
 (31) Retailleau, P.; Ducruix, A.; Ries-Kautt, M. *Acta Crystallogr.* **2002**, *D58*, 1576–1581.
 (32) Warren, P. B. *J. Phys.: Condens. Matter* **2002**, *14*, 7617–7629.
 (33) Annunziata, O.; Paduano, L.; Pearlstein, A. J.; Miller, D. G.; Albright, J. G. *J. Am. Chem. Soc.* **2000**, *122*, 5916–5928.
 (34) Albright, J. G.; Annunziata, O.; Miller, D. G.; Paduano, L.; Pearlstein, A. J. *J. Am. Chem. Soc.* **1999**, *121*, 3256–3266.
 (35) Annunziata, O.; Paduano, L.; Pearlstein, A. J.; Miller, D. G.; Albright, J. G. *J. Phys. Chem. B* **2006**, *110*, 1405–1415.
 (36) Paduano, L.; Annunziata, O.; Pearlstein, A. J.; Miller, D. G.; Albright, J. G. *J. Cryst. Growth* **2001**, *232*, 273–284.

- (37) Forsythe, E. L.; Russel, A. J.; Pusey, M. L. *J. Chem. Eng. Data* **1999**, *44*, 637–640.
 (38) Ries-Kautt, M.; Ducruix, A. F. *J. Biol. Chem.* **1989**, *264*, 745–748.
 (39) Howard, S. B.; Twigg, P. J.; Baird, J. K.; Meehan, E. J. *J. Cryst. Growth* **1988**, *90*, 94–104.
 (40) Gripon, C.; Legrand, L.; Rosenman, I.; Vidal, O.; Robert, M. C.; Boué, F. *J. Cryst. Growth* **1997**, *177*, 238–247.
 (41) Legrand, L.; Rosenman, I.; Boué, F.; Robert, M. C. *J. Cryst. Growth* **2001**, *232*, 244–249.
 (42) Tanford, C. *Physical Chemistry of Macromolecules*; Wiley: New York, 1961.
 (43) Anderson, C. F.; Courtenay, E. S.; Record, M. T., Jr. *J. Phys. Chem. B* **2002**, *106*, 418–433.
 (44) Record, M. T., Jr.; Anderson, C. F. *Biophys. J.* **1995**, *68*, 786–794.

where $\hat{\mu}_{23} = \hat{\mu}_{32}$, $\beta_{ij} = (\partial\beta_i/\partial m_j)_{m_k, k \neq j}$ and $\beta_{23} = \beta_{32}$. Protein solubility in aqueous salt solutions is typically low. Hence, the condition $Z m_2 \ll m_3$ applies for sufficiently high salt concentrations. Thus, eqs 2a–c simplify into:

$$\hat{\mu}_{22} = \frac{1}{m_2} \left(1 + Z^2 \frac{m_2}{m_3} + \beta_{22} m_2 \right) \quad (3a)$$

$$\hat{\mu}_{23} = \frac{Z}{m_3} + \beta_{23} \quad (3b)$$

$$\hat{\mu}_{33} = \frac{2}{m_3} \left(1 + \frac{\beta_{33}}{2} m_3 \right) \quad (3c)$$

Because $Z m_2 \ll m_3$, the quantity $\hat{\mu}_{33}$ can be accurately estimated from activity coefficients of the binary salt–water systems. The quantity $m_2 \hat{\mu}_{22} - 1$ is related to protein–protein thermodynamic interactions, whereas $\hat{\mu}_{23}$ is related to the protein–salt thermodynamic interaction. We note that $\hat{\mu}_{22}$ and $\hat{\mu}_{23}$ consist of a common-ion term (related to the Donnan effect) and nonideality β_{22} and β_{23} terms (mainly related to preferential solvation). The charge Z does not represent the hydrogen-ion titration charge value but the effective charge,³⁵ which includes the partial adsorption of counterions. Thus, Z is not only a function of pH but it is also a function of the nature of protein and common ion. It is also important to observe that the protein effective charge may be a function of salt concentration because chemical equilibrium occurs between free ions and binding sites. The charge dependence on salt concentration contributes to the nonideality terms, β_{22} and β_{23} . To thoroughly address the effect of salt on the thermodynamic behavior of protein solutions, it is crucial to determine the contribution of the common-ion terms and the nonideality β_{22} and β_{23} terms for protein–salt–water systems. This requires knowledge of the dependence of $\hat{\mu}_{22}$ and $\hat{\mu}_{23}$ on salt concentration.

The preferential interaction coefficients, Γ_{23} is defined by the following relation:¹³

$$\Gamma_{23} \equiv \lim_{m_2 \rightarrow 0} \left(\frac{\partial m_3}{\partial m_2} \right)_{\hat{\mu}_3} = - \lim_{m_2 \rightarrow 0} \frac{\hat{\mu}_{23}}{\hat{\mu}_{33}} \quad (4)$$

We note that, because $\hat{\mu}_{33}$ is normally known, $\hat{\mu}_{23}$ is directly related to Γ_{23} . The second virial coefficient, B_2 , is defined using statistical mechanics.⁴⁵ However, it can be also introduced from a phenomenological point of view^{42,46} using the following thermodynamic relation:

$$B_2 \equiv \lim_{m_2 \rightarrow 0} \frac{m_2 (\partial \hat{\mu}_2 / \partial m_2)_{\hat{\mu}_3} - 1}{2m_2} = \frac{1}{2} \lim_{m_2 \rightarrow 0} \left(\hat{\mu}_{22} - \frac{1}{m_2} - \frac{\hat{\mu}_{23}^2}{\hat{\mu}_{33}} \right) \quad (5)$$

The derivative $\hat{\mu}_{22}$ in the limit of small m_2 can be determined using eq 5, provided that $\hat{\mu}_{33}$ and $\hat{\mu}_{23}$ are known.

The dependence of protein solubility on salt concentration can be described by considering the phase-equilibrium condition between solution and crystal:³⁵

$$d\hat{\mu}_2 = \hat{\mu}_{22} dS_2 + \hat{\mu}_{23} dm_3 = d\hat{\mu}_{2c} \quad (6)$$

where $S_2 = m_2$ is the protein solubility and $\hat{\mu}_{2c}$ is the protein chemical potential in the crystalline phase. We can rearrange eq 6 in the following way:

$$-\frac{d \ln S_2}{dm_3} = \frac{\hat{\mu}_{23} - (d\hat{\mu}_{2c}/dm_3)}{S_2 \hat{\mu}_{22}} \quad (7)$$

Equation 7 will be used to compare our solubility data with available thermodynamic data on lysozyme–salt aqueous solutions.

Materials and Methods

Materials. Hen egg-white lysozyme, recrystallized six times and lyophilized was purchased from Seikagaku and used without further purification. Its molecular weight was assumed to be 14.3 kg mol^{-1} . We note that atomic-absorption experiments and diagnostic diffusion measurements on lysozyme–water mixtures have shown negligible amounts of low-molecular weight impurities with the exception of chloride ions, whereas no macromolecular impurity was detected by size-exclusion HPLC.³⁴ Sodium chloride, potassium chloride, and ammonium chloride were purchased from Mallinckrodt (AR grade, 99.9%) and used without further purification. Their molecular weights were assumed to be 58.44, 74.55, and 53.50 g mol^{-1} , respectively. Sodium chloride and potassium chloride were dried at $400 \text{ }^\circ\text{C}$ overnight, whereas ammonium chloride was dried at $70 \text{ }^\circ\text{C}$ for seven hours in vacuum oven.^{33–36} Deionized water was passed through a four-stage Millipore filter system to provide high-purity water for all of the experiments.

Measurements of Protein Solubility. All stock solutions used for the solubility measurements were prepared by weight to 0.1 mg. Protein–water stock solutions with protein concentration of 10–20% were prepared, and their measured pH was 4.5 or slightly higher. If necessary, pH was lowered to 4.5 by small additions of HCl aqueous solutions. Supersaturated solutions were obtained by mixing protein–water stock solutions with concentrated salt–water stock solutions. A stock solution of sodium acetate buffer (0.10 M, pH 4.5) containing 0.02% sodium azide was also added to minimize possible pH changes due to the crystallization process. The total concentration of acetate species in the final mixtures was 0.010 mol per kg of solution in all cases. The supersaturated solutions were then left at $4 \text{ }^\circ\text{C}$ (3–15 days depending on sample supersaturation) to produce crystals. The resulting suspensions were thermostatted at $25.0 \pm 0.1 \text{ }^\circ\text{C}$ under extensive stirring following a recommended procedure.⁴⁷ As crystals dissolved to reach equilibrium, the corresponding observed increase in protein concentration of the liquid phase was monitored periodically by UV absorption at 280 nm. Equilibrium was reached when the protein concentration became constant within the experimental error (5–15 days). Lysozyme molalities were calculated using the extinction coefficient of 2.64 L/g cm^{-1} at 280 nm⁴⁸ and the known partial molar volumes^{33–36} of the lysozyme–salt–water systems. The obtained experimental solubility data are available as Supporting Information. The reported errors were calculated from the maximum difference in solubility values found in the last three consecutive spectrophotometric measurements.

Results and Discussion

Lysozyme solubility, S_2 , as a function of salt molality, m_3 , for the NaCl, KCl, and NH_4Cl cases are shown in part A of Figure 1. As expected, $\ln S_2$ decreases as m_3 increases for all three cases. We can observe that the solubility curves for the NaCl and KCl cases essentially overlap within the experimental error. However the solubility curve for the NH_4Cl case is noticeably higher for $m_3 > 1 \text{ mol/kg}$. Our solubility data at $25 \text{ }^\circ\text{C}$ are consistent with solubility data previously reported at $18 \text{ }^\circ\text{C}$ on the same systems.³⁸ The effect of salt type on lysozyme solubility follows the Hofmeister series for the cations.

(45) Lebowitz, J. L. *Phys. Rev. A* **1964**, *133*, 895–899.

(46) Stockmayer, W. H. *J. Chem. Phys.* **1950**, *18*, 58–61.

(47) Asherie, N. *Methods* **2004**, *34*, 266–272.

(48) Sophianopoulos, A. J.; Rhodes, C. K.; Holcomb, D. N.; van Holde, K. E. *J. Biol. Chem.* **1962**, *237*, 1107–1112.

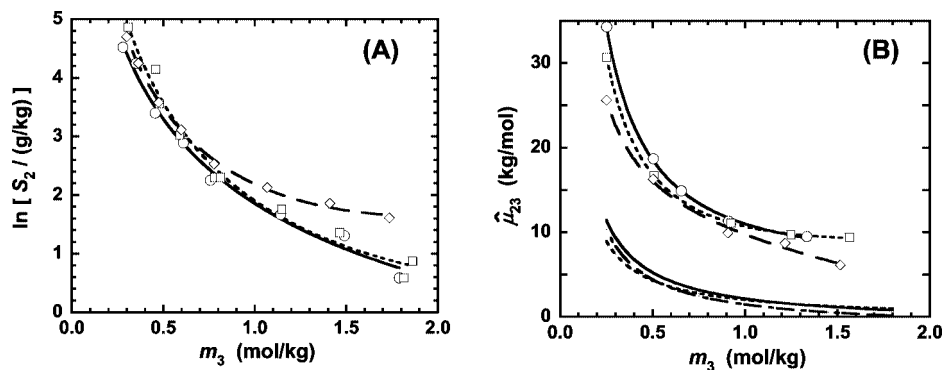


Figure 1. (A) Logarithm of lysozyme solubility, $\ln S_2$, as a function of salt concentration, m_3 , at pH 4.5 and 25 °C for NaCl (circles), KCl (squares), and NH₄Cl (diamonds). The curves (—, NaCl; ---, KCl; - · - ·, NH₄Cl) are fitted to the data using $\ln S_2 = a + b \ln m_3 + c m_3$. (B) Chemical-potential cross derivatives, $\hat{\mu}_{23}$, as a function of m_3 at pH 4.5 and 25 °C for NaCl (circles), KCl (squares), and NH₄Cl (diamonds). The curves (—, NaCl; ---, KCl; - · - ·, NH₄Cl) through the data are fits obtained using eq 3b. The curves located below the data represent the corresponding curves of $-d \ln S_2 / dm_3$ obtained using $\ln S_2 = a + b \ln m_3 + c m_3$.

At relatively high salt concentrations ($m_3 > 0.1$ mol/kg), the dependence of protein solubility on salt concentration is commonly approximated with the linear equation:^{38,49}

$$\ln S_2 = A - K m_3 \quad (8)$$

where K is the salting-out constant¹³ and A is the intercept obtained for the investigated salt concentration range. Eq 8 neglects the Debye–Huckel square-root term, which affects the solubility only at very low salt concentration. It is important to remark that the behavior of our lysozyme solubility data and previously reported data is not consistent with eq 8 (see the large deviations from linearity in part A of Figure 1).

To understand the observed experimental behavior, we examine our solubility data according to eq 7. For dilute protein solutions, we expect that $S_2 \hat{\mu}_{22} \approx 1$ (eq 3a). Thus, if we assume that the protein chemical potential in the solid phase is independent of salt concentration, eq 7 reduces to $-d \ln S_2 / dm_3 \approx \hat{\mu}_{23}$. In part B of Figure 1, we plot $\hat{\mu}_{23}$ as a function of m_3 for all three salt cases. These values, which were determined using ternary diffusion, are in very good agreement with $\hat{\mu}_{23} = 11 \pm 2$ mol/kg in 1 M NaCl previously obtained by equilibrium dialysis.⁵⁰ The high accuracy of the ternary-diffusion method has been recently tested also for polyethylene glycol in the presence of aqueous salt.⁵¹ We can see that $\hat{\mu}_{23}$ strongly depends on salt concentration in a way that resembles the observed behavior of the solubility slope. Moreover, the effect of salt type on $\hat{\mu}_{23}$ also correlates with the corresponding effect on solubility. Indeed, $\hat{\mu}_{23}$ for the NH₄Cl case is significantly lower than that for the other two cases at high salt concentration.

The experimental dependence of $\hat{\mu}_{23}$ on m_3 has been examined using eq 3b. It has been found that the common-ion term, $Z m_3$, is dominant compared to β_{23} at low salt concentrations (0.25 mol/kg) and is still about 50% of the total $\hat{\mu}_{23}$ at high salt concentrations (1.6 mol/kg). Thus, for lysozyme, these results clearly show that the common-ion effect remains very important at the higher salt concentrations relevant to crystallization protocols.¹ The common-ion effect therefore plays a significant role in determining both the dependence of protein solubility on salt concentration as well as the effectiveness of the salt as a precipitant agent.³⁵

In part B of Figure 1, we include the corresponding curves of $-d \ln S_2 / dm_3$ calculated by fitting the solubility data to $\ln S_2 = a + b \ln m_3 + c m_3$. This expression, which is based on the integration of $\hat{\mu}_{23}$ with respect to m_3 (eq 3b with the assumption that β_{23} is constant), fits very well our data (curves in part A of Figure 1). Remarkably, we can see in part B of Figure 1 that the solubility slope is only 30–40% of $\hat{\mu}_{23}$ at 0.3 mol/kg and reduces to about 10% at 1.5 mol/kg. Thus, salt effectiveness in reducing protein solubility is significantly weaker than that predicted from $-d \ln S_2 / dm_3 \approx \hat{\mu}_{23}$. We note that this analysis neglects the dependence of $\hat{\mu}_{23}$ on protein concentration. This effect is related to the change in protein concentration along the solubility boundary and is expected to become significant at low salt concentration where protein solubility is high. On the contrary, the largest observed discrepancy occurs at high salt concentrations.

According to eq 7, the discrepancy shown in part B of Figure 1 can be attributed to $S_2 \hat{\mu}_{22}$ and $(d\hat{\mu}_{22}/dm_3)$. We will now examine the deviation of $S_2 \hat{\mu}_{22}$ from unity. We can use available data on B_2 ,^{52–55} $\hat{\mu}_{23}$,³⁵ and $\hat{\mu}_{33}$,^{35,57} for the NaCl case to calculate the deviation of $\hat{\mu}_{22}$ from ideality using eq 5. Our results are shown in Figure 2. We can see that $(m_2 \hat{\mu}_{22} - 1)/m_2$ is large and positive at low salt concentrations. This behavior can be attributed to the dominant common-ion term in eq 3a. We can also see that, $(m_2 \hat{\mu}_{22} - 1)/m_2$ becomes negative at high salt concentrations. This behavior can be attributed to protein–protein attractive interactions. Nonlinear regression on $\hat{\mu}_{22}$ using eq 3a yields $Z = 6.8$ and $\beta_{22} = 237 - 599 m_3^{1/2} + 171 m_3$. The obtained value of Z is in agreement with the Z values of 6–9 obtained by applying nonlinear regression on $\hat{\mu}_{23}$.³⁵ In Figure 2, we also show the corresponding values of $S_2 \hat{\mu}_{22}$. We can see that the deviation of $S_2 \hat{\mu}_{22}$ from unity is about 50% at $m_3 = 0.3$ mol/kg and becomes lower than 10% at $m_3 \geq 0.4$ mol/kg. Although this analysis is limited to the NaCl case, similar results are expected for the other two salt cases. Thus, the

(49) Cohn, E. J. *Physiol. Rev.* **1925**, 5, 349–437.

(50) Arakawa, T.; Timasheff, S. N. *Biochemistry* **1984**, 23, 5912–5923.

(51) Tan, C.; Albright, J. G.; Annunziata, O. *J. Phys. Chem. B* **2008**, 112, 4967–4974.

(52) Lima, E. R. A.; Biscaya, E. C., Jr.; Boström, M.; Tavares, F. W.; Prausnitz, J. M. *J. Phys. Chem. C* **2007**, 111, 16055–16059.

(53) Curtis, R. A.; Ulrich, J.; Montaser, A.; Prausnitz, J. M.; Blanch, H. W. *Biotechnol. Bioeng.* **2002**, 79, 367–380.

(54) Bonneté, F.; Finet, S.; Tardieu, A. *J. Cryst. Growth* **1999**, 196, 403–414.

(55) Tessier, P. M.; Lenhoff, A. M.; Sandler, S. I. *Biophys. J.* **2002**, 82, 1620–1631.

(56) Rosenbaum, D. F.; Zukoski, C. F. *J. Cryst. Growth* **1996**, 169, 752–758.

(57) Miller, D. G. *J. Phys. Chem.* **1966**, 70, 2639–2659.

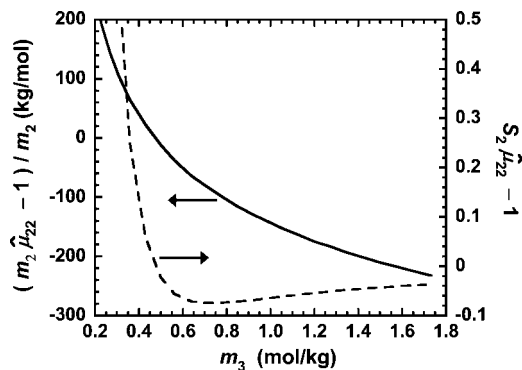


Figure 2. Deviation of Protein chemical potential from ideality, $(m_2\hat{u}_{22} - 1)/m_2$ (—), and its contribution to solubility slope, $S_2\hat{u}_{22} - 1$ (---) as a function of salt concentration, m_3 .

deviation of $S_2\hat{u}_{22}$ from unity does not account for the observed large discrepancy between solubility slope and \hat{u}_{23} . We therefore conclude that nearly all discrepancy between $-d \ln S_2/dm_3$ and \hat{u}_{23} at $m_3 = 0.4$ mol/kg or higher must be assigned to the change of protein chemical potential in the solid phase; specifically, $(d\hat{u}_{2c}/dm_3) > 0$.

That \hat{u}_{2c} is a function of salt concentration can be understood by observing that water included in protein crystals is in the range of 25–65% by weight.⁵⁸ In addition, salt ions are also found in the solid phase. Some ions are associated with particular sites in the protein crystal whereas other ions are included more irregularly. Because small ions penetrate into the solid phase,^{28,59–63} Donnan equilibrium will be established between the hydrated protein crystal and the solution.^{32,35,63} Because of the large amount of protein cations inside the crystal, an excess of chloride anions will be responsible for crystal electroneutrality as in the case of polyelectrolyte gels. Thus, \hat{u}_{2c} is expected to increase with the concentration of chloride ions in the solid phase, which, in turn, increases with m_3 in solution. In the following section, we derive a simple model for $(d\hat{u}_{2c}/dm_3)$ based on salt partitioning between solution and crystal. This model quantitatively accounts for the observed dependence of protein solubility on salt concentration.

Solubility Model. We will first report the equation describing salt partitioning based on Donnan equilibrium and then derive an expression for $(d\hat{u}_{2c}/dm_3)$. Chemical equilibrium for the salt component occurs between the two phases:⁴²

$$\hat{u}_3 = \ln m_3 + \ln(Zm_2 + m_3) + \beta_3 = \ln m_{3c} + \ln(Zm_{2c} + m_{3c}) + \beta_{3c} = \hat{u}_{3c} \quad (9)$$

where \hat{u}_{3c} is the salt chemical potential in the crystal phase, m_{2c} and m_{3c} are the molalities of protein and salt in the crystal phase, β_{3c} is the corresponding chemical-potential excess, and Zm_{2c} represents the excess of free counterions necessary to preserve electroneutrality inside the crystal. We note that Zm_{2c}

cannot be neglected with respect to m_{3c} because of the large protein concentration inside the crystal. Because Donnan equilibrium is expected to be dominant with respect to nonideality effects, we can assume that $\beta_{3c} = \beta_3$ without a significant effect on the accuracy of the model. Thus, eq 9 leads to

$$m_{3c} = [(Z/2)^2 m_{2c}^2 + m_3^2]^{1/2} - (Z/2)m_{2c} \quad (10)$$

where we have neglected Zm_2 with respect to m_3 . Eq 10 describes salt partitioning between solution and the hydrated crystalline phase.

Protein molality in the crystalline phase does not change significantly with the composition of the liquid phase. Thus, $(d\hat{u}_{2c}/dm_3)$ can be expressed as a product of two partial derivatives:

$$\frac{d\hat{u}_{2c}}{dm_3} = \left(\frac{\partial \hat{u}_{2c}}{\partial m_{3c}} \right)_{m_{2c}} \left(\frac{\partial m_{3c}}{\partial m_3} \right)_{m_{2c}} \quad (11)$$

As shown for \hat{u}_2 (eq 2a), $(\partial \hat{u}_{2c}/\partial m_{3c})_{m_{2c}}$ is given by:

$$\left(\frac{\partial \hat{u}_{2c}}{\partial m_{3c}} \right)_{m_{2c}} = \left(\frac{\partial \hat{u}_{3c}}{\partial m_{2c}} \right)_{m_{3c}} = \frac{Z}{Zm_{2c} + m_{3c}} + \beta_{23} \quad (12)$$

where we have assumed that the relatively small nonideality term in eq 12 is the same as that of eq 3b. The expression for $(\partial m_{3c}/\partial m_3)_{m_{2c}}$ can be derived from eq 10:

$$\left(\frac{\partial m_{3c}}{\partial m_3} \right)_{m_{2c}} = \frac{2m_3}{Zm_{2c} + 2m_{3c}} \quad (13)$$

Combination of eqs 10–13 yields:

$$\frac{d\hat{u}_{2c}}{dm_3} = \frac{Z}{m_3} \frac{(1 + \alpha^2)^{1/2} - 1}{(1 + \alpha^2)^{1/2}} + \beta_{23} \frac{\alpha}{(1 + \alpha^2)^{1/2}} \quad (14)$$

where $\alpha \equiv 2m_3/(Zm_{2c})$. We are now in position to write an expression for $-d \ln S_2/dm_3$ using eq 7 with the assumption that $S_2\hat{u}_{22} = 1$:

$$-\frac{d \ln S_2}{dm_3} = \frac{Z}{m_3} \frac{1}{(1 + \alpha^2)^{1/2}} + \beta_{23} \frac{(1 + \alpha^2)^{1/2} - \alpha}{(1 + \alpha^2)^{1/2}} \quad (15)$$

Thus, according to eq 15, the characterization of solubility slope requires only one additional parameter represented by the protein molality, m_{2c} , inside the hydrated crystal. Integration of eq 15 with respect to m_3 yields:

$$\ln S_2 = A + Z \tanh^{-1} \frac{1}{(1 + \alpha^2)^{1/2}} + \beta_{23} \frac{(1 + \alpha^2)^{1/2} - \alpha}{(2/Zm_{2c})} \quad (16)$$

where A is the integration constant.

To compare eq 16 with our solubility data in part A of Figure 1, we determine A by assuming that $\ln S_2 = 1.9$ at $m_3 = 1$ kg/mol. For Z and β_{23} , we use the values of 7 and 3.5 mol/kg, respectively. These parameters are consistent with the experimental values of \hat{u}_{23} as shown by the calculated curve in part A of Figure 3. In part B of Figure 3, we plot $\ln S_2$ as a function of m_3 for three different values of m_{2c} . These m_{2c} values are chosen to be of the same order of magnitude as the typical protein concentrations inside the crystal.^{58,61} As we can see in the figure, eq 16 describes quite well the experimental behavior of solubility within the experimental concentration domain. For comparison, we also show the solubility curve calculated using $\ln S_2 = A - Z \ln m_3 - \beta_{23}m_3$, based on the assumption that $(d\hat{u}_{2c}/dm_3) = 0$. We can see that this curve

(58) Matthews, B. W. *J. Mol. Biol.* **1968**, *33*, 491–497.

(59) Vaney, M. C.; Maignan, S.; Riès-Kautt, M.; Ducruix, A. *Acta Crystallogr.* **1996**, *D52*, 505–517.

(60) Vaney, M. C.; Broutin, I.; Retailleau, P.; Douangamath, A.; Lafont, S.; Hamiaux, C.; Prange, T.; Ducruix, A.; Riès-Kautt, M. *Acta Crystallogr.* **2001**, *D57*, 929–940.

(61) Morozova, T. Y.; Kachalova, G. S.; Evtodienko, V. U.; Botin, A. S.; Shlyapnikova, E. A.; Morozov, V. N. *Biophys. Chem.* **1996**, *60*, 1–16.

(62) Vekilov, P. G.; Monaco, L. A.; Thomas, B. R.; Stojanoff, V.; Rosenberger, F. *Acta Crystallogr.* **1996**, *D52*, 785–798.

(63) Chang, J.; Lenhoff, A. M.; Sandler, S. I. *J. Phys. Chem. B* **2005**, *109*, 19507–19515.

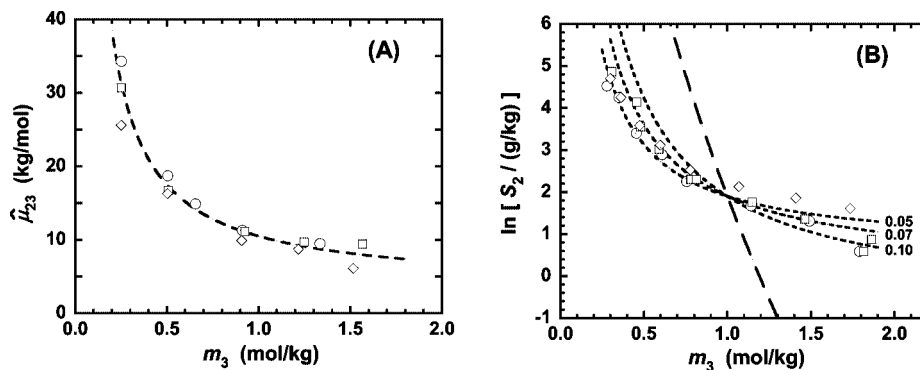


Figure 3. (A) Experimental data of part B of Figure 1 and $\hat{\mu}_{23}$ curve (---) calculated using eq 3b with $Z = 7$ and $\beta_{23} = 3.5$ mol/kg as a function of salt concentration, m_3 . (B) Experimental data of part A of Figure 1 and three $\ln S_2$ curves (---) calculated using eq 16. The numbers associated with the three curves represents the corresponding values of m_{2c} (mol/kg). A fourth curve (---) represents $\ln S_2$ calculated by assuming that $(d\hat{\mu}_{23}/dm_3) = 0$.

is significantly steeper than the experimental data in contrast with the curves based on eq 16.

Comments on Common-Ion Effect and Protein Solubility. It is well-known that the aqueous solubility of an ordinary salt can be reduced by the addition of another, more soluble salt with a common ion.⁶⁴ In this case, the crystalline phase is essentially a pure neutral component and the common-ion effect leads to a solubility decrease that is inversely proportional to the concentration of the soluble salt. However, protein crystals are permeable to salts, and common ions do not necessarily cocrystallize with the proteins. This implies that the common-ion effect is relatively weak in the case of (charged) proteins. This is consistent with chloride salts being found to be ineffective in reducing solubility for many protein cases. In such cases, kosmotropic precipitants^{18,65} such as $(\text{NH}_4)\text{SO}_4$ are usually employed in protein crystallization protocols.¹ Nonetheless, it is intriguing that chloride salts are very successful at inducing lysozyme crystallization. In the data detailed above, the dominant role of the common-ion effect on lysozyme solubility suggests that the enhancement of this effect in other

protein cases may lead to a rationale development of new protocols for protein crystallization.

Conclusions

Comparison between lysozyme solubility in the presence of aqueous chloride salts and thermodynamic data of the corresponding solutions demonstrate that most of the discrepancy between $-d \ln S_2/dm_3$ and $\hat{\mu}_{23}$ must be assigned to $(d\hat{\mu}_{23}/dm_3) > 0$. A model based on salt partitioning between the solution and the hydrated crystalline phase quantitatively accounts for the observed dependence of protein solubility on salt concentration. A better understanding of common-ion effects will be valuable for a rational design of new conditions for protein crystallization.

Acknowledgment. We thank John G. Albright for valuable comments on the manuscript. This work was supported by the ACS Petroleum Research Fund (47244-G4) and TCU Research and Creative Activity Funds.

Supporting Information Available: Experimental solubility data. This material is available free of charge via the Internet at <http://pubs.acs.org>.

JA804304E

(64) Pauling, L. *General Chemistry*; Dover: New York, 1970.

(65) Chen, X.; Yang, T.; Kataoka, A.; Cremer, P. S. *J. Am. Chem. Soc.* **2007**, *129*, 12272–12279.